# Enhanced adsorption of Congo red dye by CS/ZnO nanocomposite: Synthesis, characterization and performance evaluation

**Dhawan Monika[1], Yadav Sashi[1], Kumar Vineet[1], Bala Kiran[2] and Chhikara Sunil Kumar[1]***
1. UIET, Maharshi Dayanand University, Rohtak-124001, Haryana, INDIA
2. KLP College, Rewari- 123401, Haryana, INDIA
*sunilchhikara.uiet@mdurohtak.ac.in

***Abstract***
*The need for effective and sustainable techniques to remove dye contamination from various ecosystem has been identified by increasing concerns about environmental pollution. This study synthesized novel zinc oxide nanocomposite derived from crab shell (CS/ZnO). Field emission scanning electron microscopy (FE-SEM), Fourier transform infrared spectroscopy (FTIR), X-ray diffraction (XRD) and Zeta potential were used to characterize the nanocomposite structure. Batch adsorption studies were used to determine the congo red (CR) adsorption effectiveness utilizing adsorbent dose, contact duration, pH and temperature variables. The maximum adsorption capacity (qmax) of 62.88 mg/g CS/ZnO composite was consistent with the Langmuir model based on the data obtained for CR adsorption equilibrium. The kinetics study verified that the pseudo 2nd order rate kinetic model was most effective and the qmax was evaluated at pH 6.0 and 90 minutes.*

*Thermodynamic analysis exposed that the adsorption phenomenon was endothermic, spontaneous and physical in nature. The protonation of the -$NH_2$ groups in the CS/ZnO composite, which increased its electro-positivity, is primarily responsible for the high adsorption efficiency. The adsorption mechanism is controlled by the creation of hydrogen bonds and electrostatic attraction between dye and nanocomposite. The CS/ZnO composite may be regarded as an effective, advantageous and promising adsorbent for environmental cleanup.*

**Keywords:** Congo red, Crab shell, Zinc oxide, Adsorption.

## Introduction

All living things on the Earth depend upon water resources for their survival and it is generally believed that water is the basic need of life. Although water makes up 71% of the Earth's surface, in which only fresh water can meet the needs of various plant, animal and human species, that accounts for 2.5% of the total water resources. However, 1.6 billion people around the world suffer from water scarcity and dearth of access to clean water due to a number of factors like industrialization, rapid urbanization, population growth, unrestricted resource exploitation, prolonged droughts and an over reliance on the groundwater[12,36,37].

Nowadays, environmental contamination is regarded as a serious global problem. Toxic wastewater generated by different processes has a detrimental effect on soil fertility, aquatic life, ecosystem integrity and water resources[16]. Furthermore, previous surveys have shown that more than 80% of polluting industrial effluent is discharged into the environment untreated, potentially contaminating water sources. Artificial dyes are the main contaminants of aqueous solutions used in many industries[24,33].

Numerous contaminants, such as dyes, are discharged into the environment untreated, disrupting the ecosystem and endangering both human and environmental health. There are over 100,000 different varieties of commercial dyes, over $7 \times 10^5$ tons of dye are manufactured annually world-wide and the food and textile sectors discharge significant amounts of dyes into the environment[22]. The textile dyeing industry is responsible for around 15–20% of water pollution and dyes are regarded as important pollutants in wastewater due to their toxicity at extremely low concentrations (<1 ppm)[8,14].

One common anionic azo dye that has been used extensively is Congo red (CR), which is inherently toxic to living things. Hazardous organic wastewater which is hard to break down and requires a lot of chemical oxygen, is CR-containing wastewater because of its complex aromatic structure and thermal stability. Furthermore, benzidine, a known carcinogen, is the breakdown product under anaerobic circumstances[43]. Therefore, for sustainable growth, excessive CR in wastewater must be eliminated using eco-friendly methods.

Recently, coagulation, membrane separation, adsorption and photocatalytic degradation have been applied as traditional techniques to remove dyes from wastewater. Adsorption is the most economical and environmentally favorable technique for color degradation, out of all the known treatment options. Because of its natural availability, affordability, biocompatibility, biodegradability and minimal or nonexistent toxicity, chitosan is a very desirable material for adsorption applications[38]. Chitosan is a naturally occurring polymer that is produced when chitin undergoes alkaline deacetylation. Chitin is a widely accessible biopolymer that is mostly found in the exoskeleton of insects, fungi and crustaceans like prawns and crabs[30].

Because of the reactive hydroxyl and amine group in its backbone, which serve as active site for the removal of metal contaminants as well as both anionic and cationic dyes, chitosan offers exceptional chelating and adsorption capabilities in addition to the previously stated ones. However, chitosan's use is limited by a few disadvantages, including its low specific surface area, low mechanical resistance and solubility in acidic conditions. Chitosan has therefore been altered using a variety of methods, including crosslinking reagents, grafting functional group onto the chitosan structure, improving the adsorption capability and functionalization to create composites, in order to get around these drawbacks and enhance the adsorbent performance[2]. In addition to stabilizing chitosan in acidic solutions, crosslinking agents such as epichlorohydrin, formaldehyde, tripolyphosphate, glutaraldehyde, sodium and glyoxal also enhance its mechanical qualities[22].

Combining two or more resources with different chemical and physical properties results in composite materials. Ceramic material as (oil palm ash, polyurethane, montmorillonite, bentonite, activated clay and kaolin), magnetic chitosan composite with magnetic material for easy pollutant separation and other hybrid composites or nanocomposite with metal oxide nanoparticle ($TiO_2$, ZnO, $SiO_2$, SnO) and graphene are just a few of the many materials used to prepare composites with chitosan.

The current work is focused on the synthesis of CS based ZnO nanocomposite utilizing microwave assisted technique in order to fill in the existing research gaps. Since several different colorants are often used in the dyeing process, the effluents from textile manufacturing companies typically contain a wide variety of complex dyestuffs. Decolorization is a difficult procedure due to the presence of various functional group or dye classes in the textile effluent might alter the removal rate[27].

As wasted dye baths are a major environmental hazard, it is imperative that sustainable process-based methods should be developed for their eco-efficient decontamination. In the present study, nanocomposite was prepared from chitosan and zinc oxide. This study explores the use of these composites as adsorbent to treat dye wastewater. The objectives of the study are as follows: preparation of nanocomposite and their characterization; and to study the effect of several parameters such as contact time, pH, adsorbent dose and temperature in batch study on congo red dye removal.

## Material and Methods

Chitosan (extracted from crab shells) was obtained from Marine Chemicals, India. Zinc oxide nano-powder and glacial acetic acid were obtained from Techinstro, India. Congo red (CR) dye was obtained from the Lobachemie. Sodium hydroxide pellets (NaOH) and hydrochloric acid (HCl) were obtained from Fischer Scientific. Double distilled water was used for the preparation of all the solution.

**Preparation of CS/ZnO nanocomposite:** The chemical reaction between crab shell and zinc oxide was conducted in a domestic microwave oven. Total 2.0 g of zinc oxide-NP was dissolved in 200 ml of double distilled water (solution 1). Then, 2.0 g of chitosan was dissolved in 200 ml of 1% acetic acid solution (solution 2). A round flask with a quick fit bottom was used to stir the mixture solutions of 1 and 2.

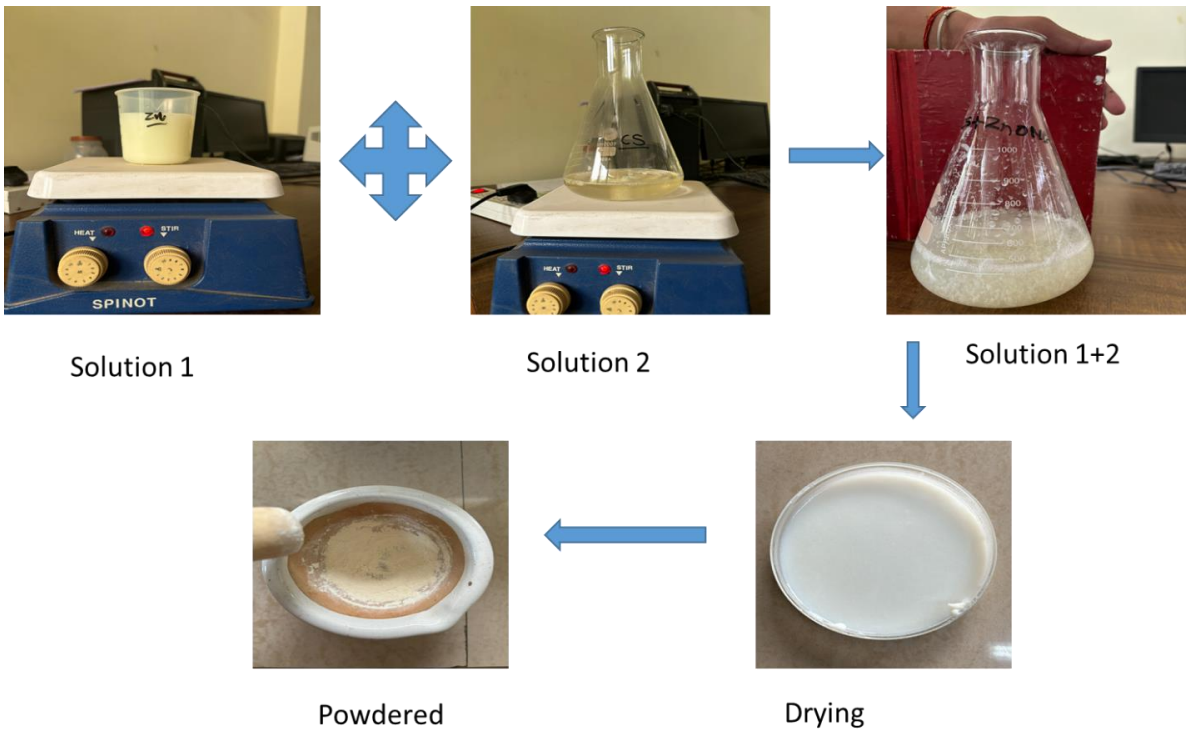


**Figure 1: Synthesis process of crab shell-zinc oxide nanocomposite**

After adjusting for 15min contact time, flask was placed inside microwave-oven. After fifteen minutes, the reaction was examined. Decantation and washing with distilled water were done to get rid of the unreacted material and to get the product at the end of the reaction. The product was vacuum oven dried until its weight remained constant. The unreacted chitosan material was then precipitated by filtering the extracted solution and adjusting the filtrate to pH 9. The precipitate was washed and dried properly[23].

**Characterization of Nanocomposite:** The surface characterization of nanocomposite for presence of functional groups was carried out with the help of FTIR spectroscopy by using Bruker Alpha model FTIR spectrometer fitted with OPUS software (Department of Biotech Engineering, UIET, Maharshi Dayanand University, Rohtak). The samples were used in powdered form for FTIR analysis. The spectra were captured in the 400 $cm^{-1}$ to 4000 $cm^{-1}$ range. Particle size as well as Zeta potential of nanocomposite was determined by Zetasizer (Malvera) available at the Central Instrumentation Laboratory (CIL), Maharshi Dayanand University, Rohtak. Surface morphology and elemental analysis of nanocomposite were done using FE-SEM, 7610F Plus/ JEOL and Energy Dispersive Spectroscopy. An XRD instrumentation was used to observe the crystalline structure of the nanocomposite in the wide-angle region (10–80°). When electrons strike a solid sample, XRD produces X-rays. By hitting a crystal structure, distinct X-ray behavior can be investigated[39].

**Batch adsorption study:** The batch adsorption experiment was conducted in triplicate using 50 mL of solution containing 5-50 mg of adsorbent, with initial dye concentration (20 mg $L^{-1}$), contact time (15min–120min), pH (2.0–9.0) and temperature (15˚C– 45˚C) parameters. The studies included variations in temperature, pH, contact duration and adsorbent dosage. The 1M HCl solution and 1 M NaOH solution were added to change its pH. Following the adsorption procedure, the dye concentrations at a wavelength of 498 nm were measured using a UV-Vis spectrophotometer. Equations 1 and 2 are used to calculate the adsorption capacity of the adsorbent and the removal efficiency of CR.

$$Adsorption\ (\%) = \frac{c_o - c_e}{c_o} \times 100 \quad (1)$$

$$q_e = \frac{c_o - c_{e \times V}}{m} \quad (2)$$

where qe, $C_o$, $C_e$, V and m stand for equilibrium adsorption-capacity in mg $g^{-1}$, adsorbate's initial concentration in mg $L^{-1}$, the adsorbate's equilibrium concentration in mg $L^{-1}$, adsorbate solution's volume in ml and adsorbent's mass in mg respectively[40].

## Results and Discussion

**Characterization of CS/ZnO:** CS/ZnO nanocomposite synthesized has been observed using UV-vis spectroscopy. The UV-vis spectrophotometer absorbance peak of the synthesized CS/ZnO nanocomposite was observed at around 360 nm. One of the distinctive characteristics of ZnO particles is the presence of a UV–visible absorbance spectrum at about 360 nm. According to Dananjaya et al[7], the chitosan-coated ZnO nanocomposite's UV–visible absorbance spectrum was detected at 355 nm. The microwave heated chitosan stabilized zinc oxide nanoparticles also showed a high UV–visible absorption peak at 360 nm[5,25].

The synthesized CS/ZnO nanocomposite's average particle size was 78.42 nm, according to the DLS particle size distribution data, while the range of particle sizes was 20–150 nm (Fig. 2a). The size determined by FE-SEM and the DLS findings is consistent. The Zeta sizer was used to measure surface charge on the CS/ZnO nanocomposite. The produced nanocomposite's positive surface charge value (+35.6 mV) is shown in fig. 2b. Since chitosan is a positively charged biopolymer, the positive value from the zeta sizer data further confirms that chitosan is present on surface of produced nanocomposite. Wu et al[35] reported similar results, indicating that the produced CS/ZnO nanocomposite has a positive surface charge.

Figure 3 depicted the synthesized CS/ZnO nanocomposite's FTIR spectrum before and after adsorption. The IR peak at 3851, 3743 $cm^{-1}$ in the measured spectra is attributed to C-H and -OH stretch vibrations of phenols and carboxylic acids. The C-H, C=O and -OH stretches represented by the FTIR spectra bands at 3344, 2939 and 2357 $cm^{-1}$ suggest the potential existence of alcohols, esters, carboxylic acids and phenols. The presence of amine (N-H bend), aliphatic amine (C=O stretch) and carboxylic acid (C-H bend, C-N stretch) was attributed to the IR peaks at 1744, 1509, 1388 and 1035 $cm^{-1}$. The C-H and N-H bend suggest the potential presence of phenolic acids, carboxylic groups, alcohols, free hydroxyl and amines.

The other peaks, which were found at about 941, 825, 656 $cm^{-1}$, were attributed to the –OH bend. Several phenolic acids, carboxylic acids and amines were found to be present, based on the FTIR study. The chitosan polymer may be used to detect additional functional groups of amine ($-NH_2$). These functional groups might serve as capping and reducing agents during the manufacture of the CS/ZnO nanocomposite. The occurrence of newer peak at 1699.29 $cm^{-1}$ is assigned to aromatic skeletal vibration of congo red dye molecule[13].

FE-SEM analysis was used to characterize morphological characteristic of synthesised CS/ZnO nanocomposite. In accordance with Yusof et al[41], the produced CS/ZnO nanocomposite was shown to have an agglomerated spherical nanoparticle with an average size of 47–70nm by FE-SEM image (Fig. 4). The produced CS/ZnO nanocomposite's morphology exhibited a spherical form with an average size of 25 to 70nm, which is consistent with our results[4]. The chitosan nanoparticles enclosed in synthetic

6-Thioguanine have a spherical form[26]. The loading of congo red on surface of the nanocomposite after adsorption has caused the visual appearance to shift into an irregular and heterogeneous surface (Fig. 4c, 4d). Adsorbed congo red molecules of different sizes cause the polymeric surface to become rougher and more irregular.

CS/ZnO nanocomposite component were found by energy dispersive X-ray spectroscopy (EDS). The elements oxygen (38.6%), carbon (28.7%) and zinc (27.4%) are present in the synthesized composite, according to the EDS spectra (fig. 4e). The existence of CS in the CS/ZnO composite is supported by the detection of O as well as Zn which shows the production of ZnO particles. The carbon concentration increases after congo red adsorption, likely as an outcome of carbon attachment. The adsorption of congo red on surface of the chitosan-ZnO nanocomposite was confirmed by the presence of sulfur associated with the structure of congo red (Fig. 4c).

The immobilization of ZnO nanoparticle on chitosan was examined by X-ray diffraction. The XRD pattern of the synthesised CS/ZnO nanocomposite is depicted in fig. 5a. The XRD pattern of the synthesised CS/ZnO nanocomposite following congo red adsorption is depicted in fig. 5b. XRD analysis was used to determine the crystalline structure of synthesised CS/ZnO nanocomposite. In addition to matching JCPDS card no. 36–1451, the peaks at 2θ value of 31.9°, 34.5°, 36.4° and 62.9° correspond to the crystal planes of (100), (002), (101) and (103) respectively. These planes are linked to a wurtzite structure with hexagonal phase of ZnO[3]. Bharathi et al[5] reported similar results. The findings showed that ZnO hexagonal phase has been successfully immobilized on chitosan.

**Adsorption study:** The synthesized Cs/ZnO nanocomposite was used for adsorption of congo red dye. For dye optimization of parameters, batch study was used. The various parameters used were pH, dosage, time and temperature. Effects of all these parameters were studied by varying one variable and others keeping constant. One of the parameter having noteworthy impact on adsorption capacity is pH, which plays crucial role by regulating the adsorbent charge and the degree of adsorbate ionization in solution. With all other parameters held constant, the effect of solution pH on CR dye adsorption was examined in range of 2.0–9.0. The impact of pH on the dye's rate of adsorption onto the nanocomposite surface is depicted in fig. 6.

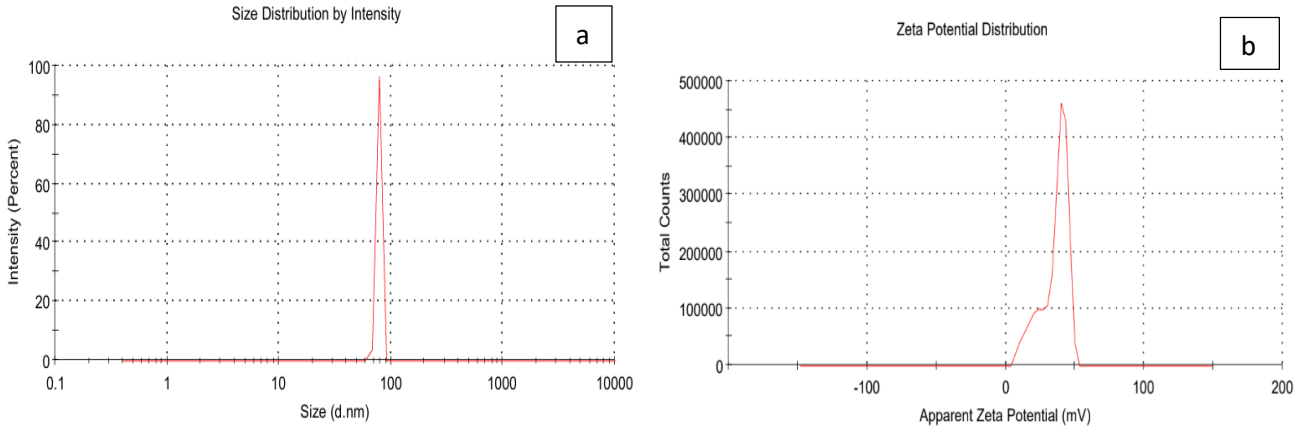


**Figure 2: (a) Size distribution and (b) zeta-potential of CS/ZnO nanocomposite**

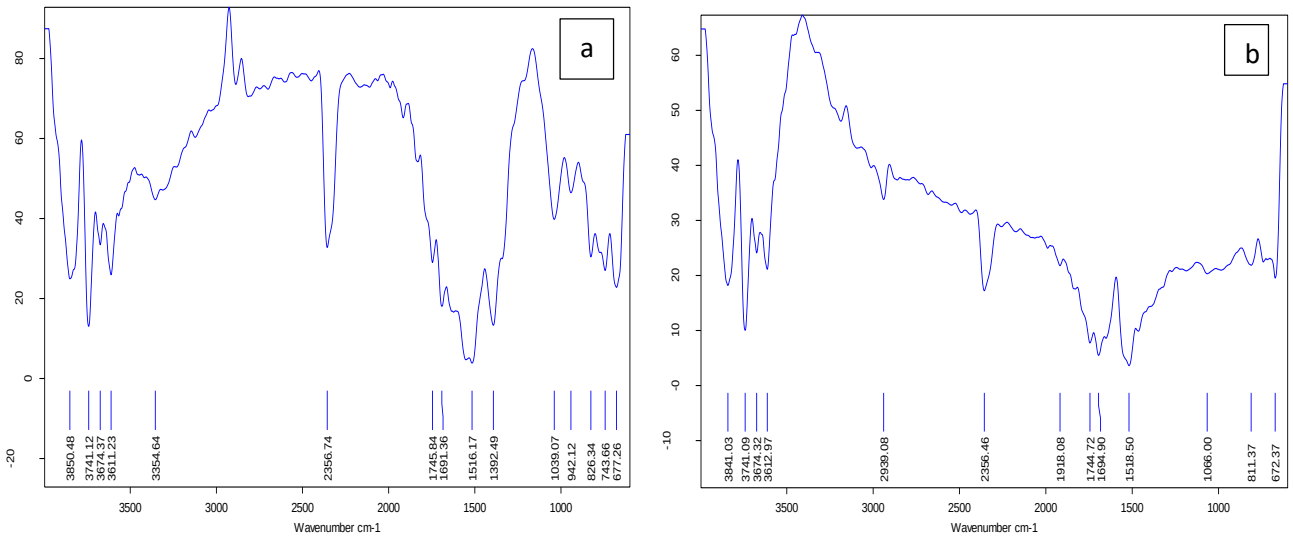


**Figure 3: (a) FTIR spectra of CS/ZnO before adsorption, (b) after congo red adsorption**

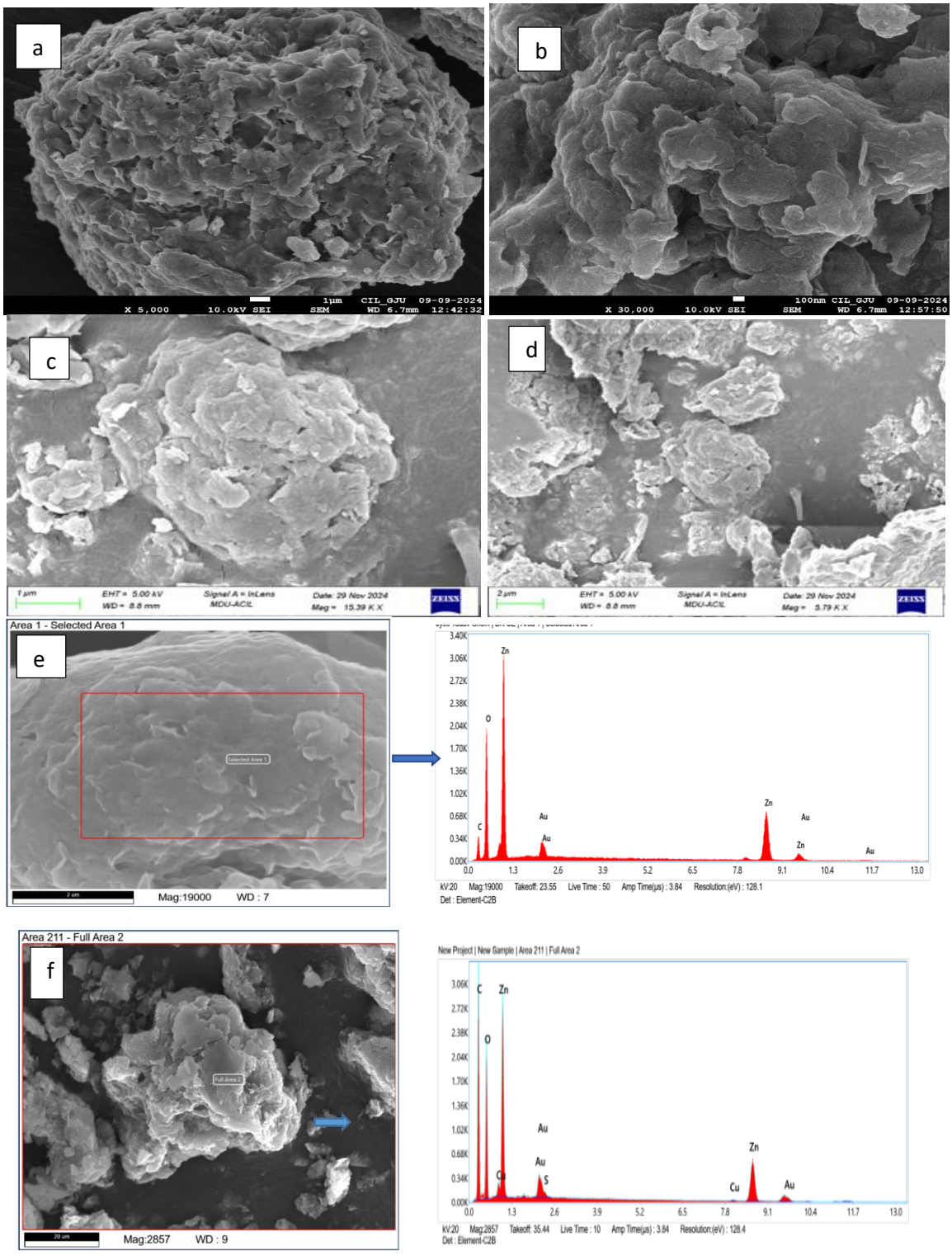


**Figure 4: (a) FESEM at 1µm and (b) 100nm, before adsorption; (b) and (c) after congo red adsorption; (e) EDS of synthesized CS/ZnO nanocomposite before adsorption and (f) after congo red adsorption**

Because of the protonation of the hydroxyl, SiO and amino groups on surface of the nanoparticle, the removal capacity for CR dye rose from 2.0 to 6.0 before decreasing as the pH of the solution ascended further. At pH 6.0, CR dye maximum adsorption capacity was 65.43 mg $g^{-1}$. Therefore, the ideal pH for further adsorption trials was determined to be 6.0 for CR dye and similar outcomes have also been documented by Roy et al[29]. The dye molecules and the hydrogel film surface are very electrostatically repelled at low pH values. The competition among dye and $H^+$ ions for the available adsorption sites limits the adsorption capacity[31]. Dyes feature active sites that allow them to bind to the hydrogel film and attain the higher adsorption efficiency at the right pH. In order to progress adsorption efficiency, further adsorption tests were carried out for CR dye at pH 6.

The adsorbent dosage is one of the factors that significantly affects sorption capacity. It provides binding site and a sizable surface area for adsorption of dye on the adsorbent. While initial dye concentration (20 $mgL^{-1}$), contact period (90 minutes) and pH 6.0 were held constant, the impact of dosage was investigated in range of 5.0 mg to 50.0 mg in 50.0 mL of adsorbate solutions. As the adsorbent dosage rises, the adsorption capacity for CR drops from 170.58 to 18.73 mg $g^{-1}$ as depicted in fig. 7. This results in a decrease in dye by an adsorbent-mass unit because certain adsorption sites were left vacant, caused by more availability of exchangeable sites at higher adsorbent dose or surface area[1].

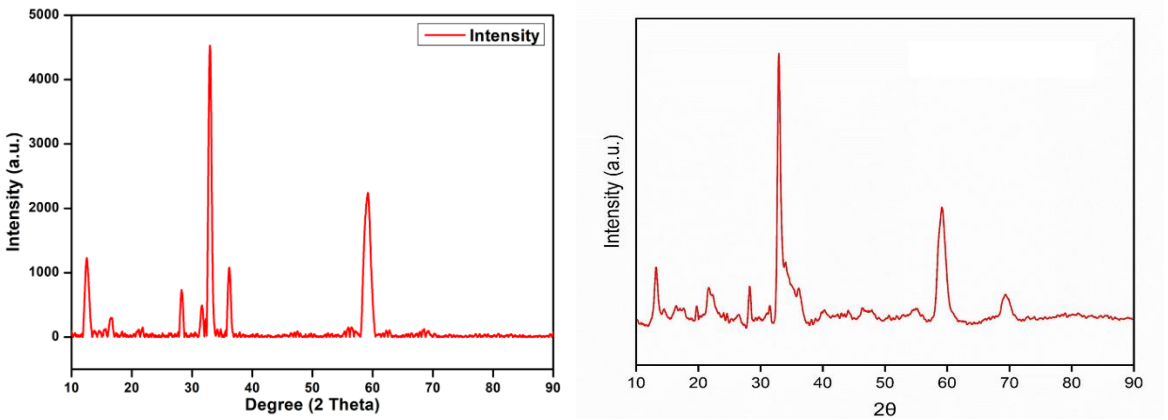


**Figure 5: (a) XRD of synthesised CS/ZnO nanocomposite, (b) After congo red adsorption**

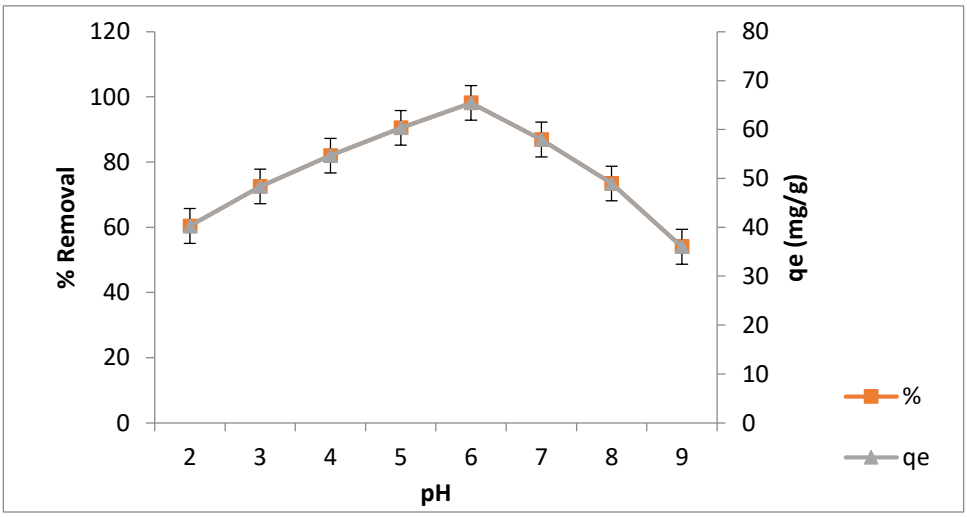


**Figure 6: Effect of pH on congo red adsorption by CS/ZnO**

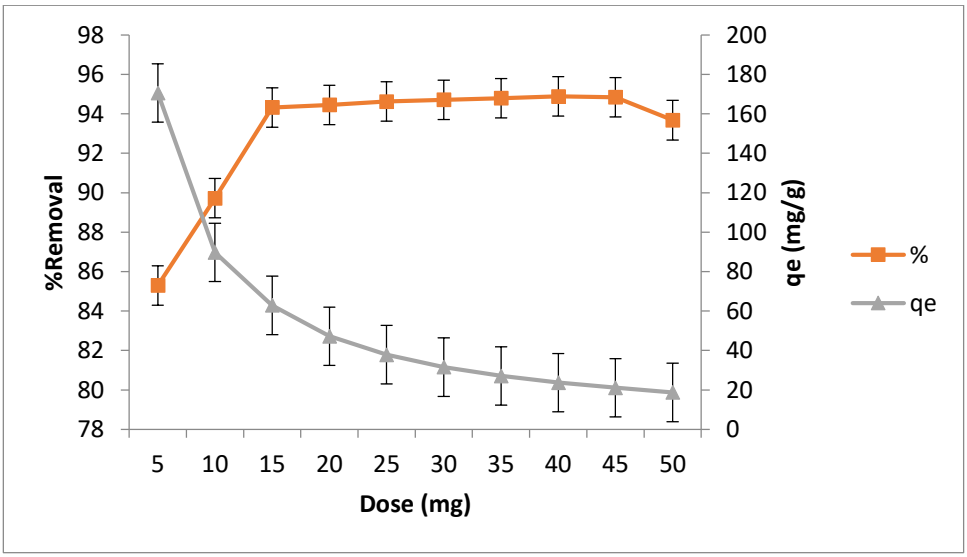


**Figure 7: Effect of adsorbent dose on congo red adsorption by CS/ZnO**

Contact time is a crucial factor in an adsorption experiment that has a direct impact on the kinetics of adsorption. The effects of contact time (15–120 min) on CR adsorption onto the adsorbent surface were investigated at a constant pH of 6.0 for CR dye, dose of 15.0 mg and temperature of 25°C (Fig. 8). Due to the abundance of active sites on the nanocomposite surface, the adsorption process started out very quickly. Once equilibrium was reached, dye molecules had to compete for the available adsorption sites. After 90 minutes, the equilibrium for CR adsorption was reached. The adsorption capacity does not alter over time once equilibrium is achieved. As a result, 90 minutes was chosen as the ideal duration for CR dye adsorption.

The effect of temperature on congo red removal between 15˚C and 45˚C is shown in fig 9. The congo red molecules motion is improved by the higher temperature which raises the removal percentage. Additionally, a higher temperature promotes a stronger chemical bond between the nanocomposite and congo red, which increases removal efficiency. Molecules move more quickly and with greater kinetic energy at higher temperatures. This quick transport favors improved adsorption by increasing the collision between congo red and the nanocomposite. At 25˚C, the removal efficiency reaches its maximum. As a result, the ideal temperature for congo red removal is 25˚C. After reaching 25˚C, the removal efficiency stays constant, indicating that equilibrium has been reached. However, more active sites are available and a constant removal rate is achieved at higher temperatures.

**Isotherm, kinetic and thermodynamic study:** In order to investigate the distributions of adsorbate in adsorbent (solid phase) and aqueous solution (liquid phase), the experiment data was examined by adsorption isothermic model. The adsorption models of Temkin, Freundlich and Langmuir were studied for the fitment to the experimental data. Monolayer adsorption takes place according to Langmuir isotherm model which assumes that adsorbent surface has uniform adsorption site with equal energy[20]. The energy of the adsorption site in the Freundlich model, on the other hand, is nonuniform and collapses exponentially as the adsorption coverage increases[11]. In contrast to these two models, T-K models take temperature effects into account[9,28].

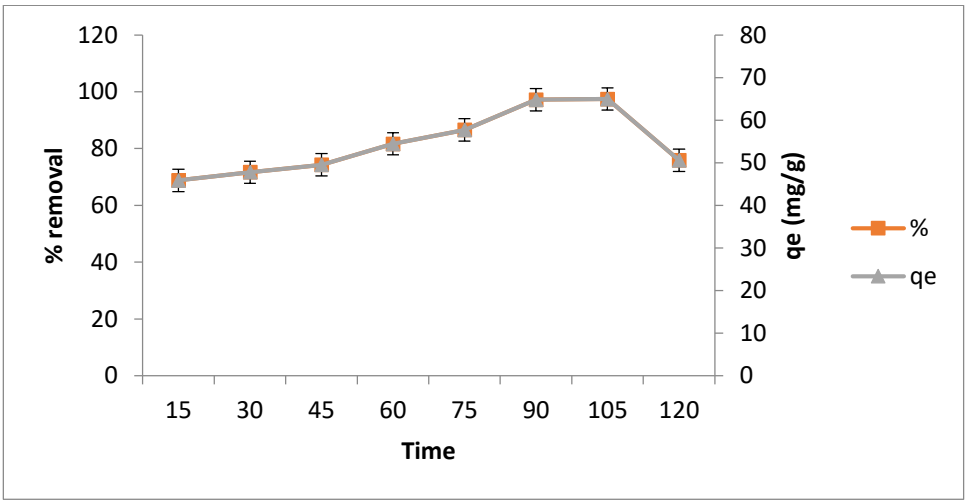


**Figure 8: Effect of contact time on congo red adsorption by CS/ZnO**

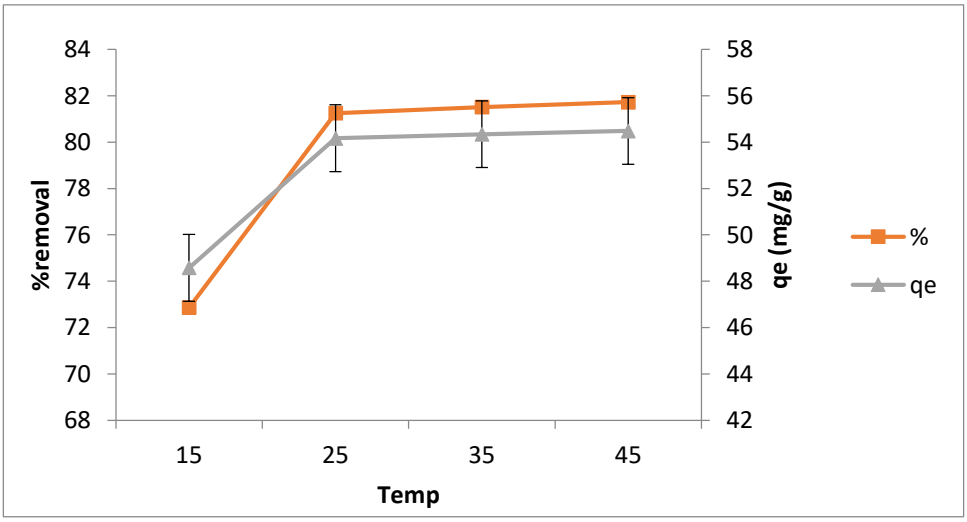


**Figure 9: Effect of temperature on congo red adsorption by CS/ZnO**

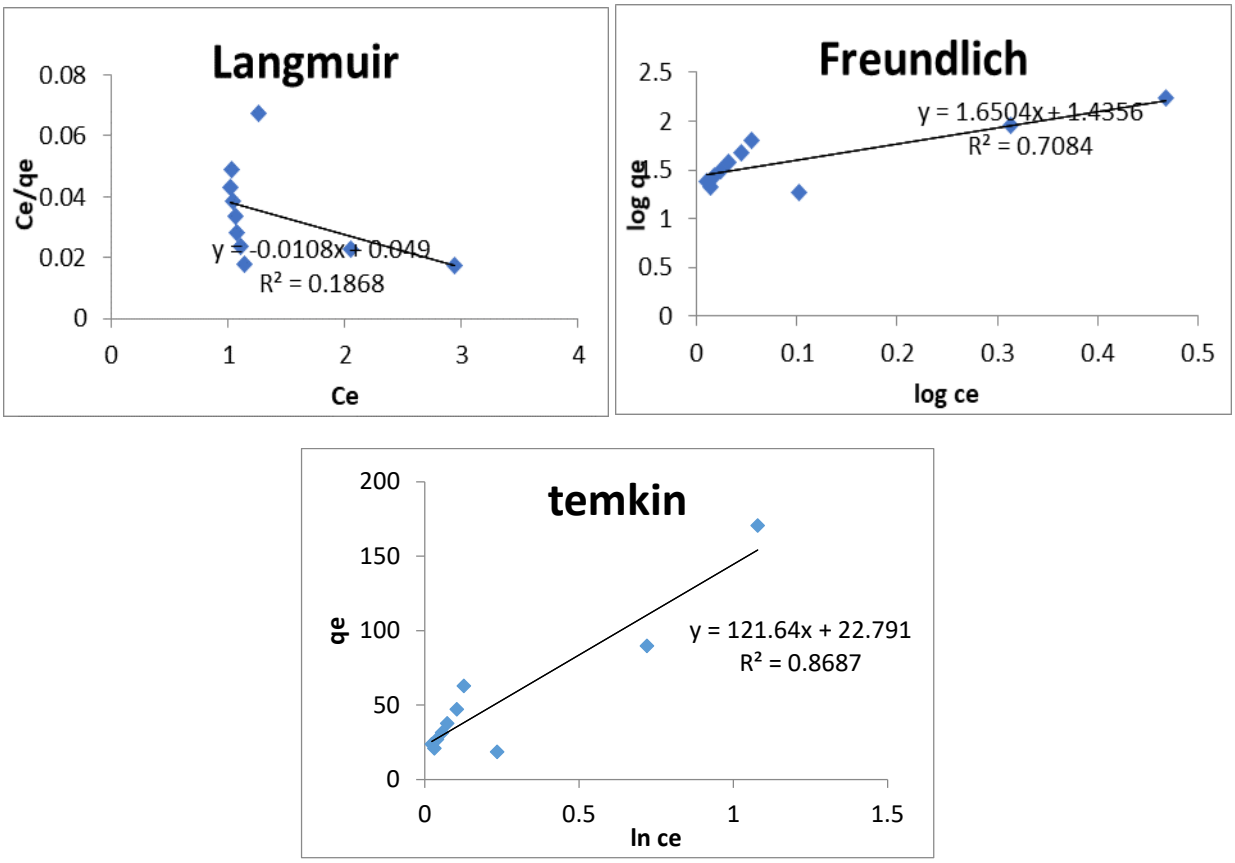


**Figure 10: Langmuir, Freundlich and Temkin isotherm for congo red adsorption by CS/ZnO**

**Table 1**
**Isothermic parameters**

| | | |
|---|---|---|
| Langmuir | $Q_m$ | 92.592mg $g^{-1}$ |
| | B | 4.444 |
| | $R_L$ | 0.0111 |
| | $R^2$ | 0.18 |
| Freundlich | N | 0.606 |
| | $K_f$(L/g) | 26.91 |
| | $R^2$ | 0.7 |
| Temkin | bT | 0.0203 |
| | BT | 121.64 |
| | AT | 1.2060 |
| | $R^2$ | 0.86 |

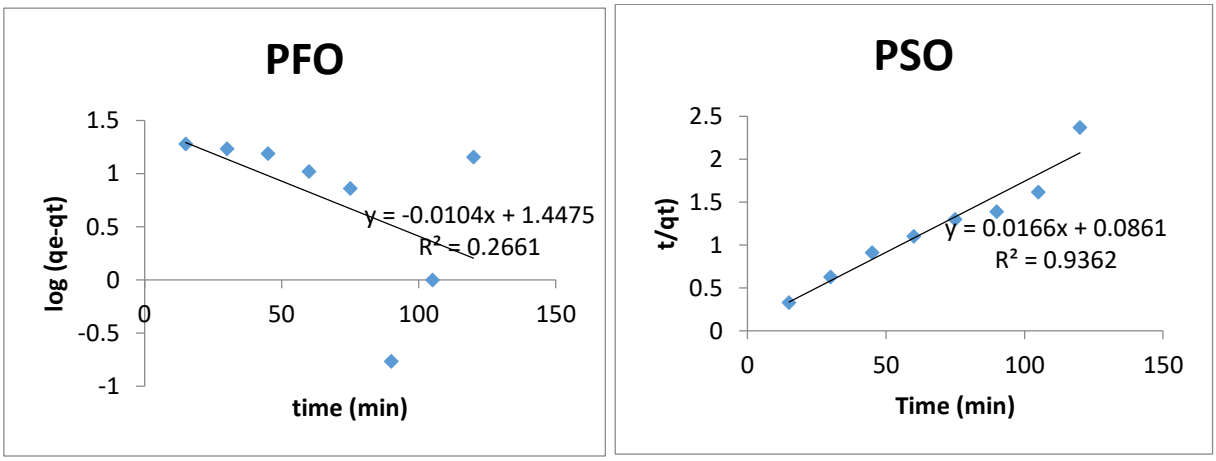


**Figure 11: Pseudo first order and Pseudo second order rate kinetics**

The adsorption experimental data was fitted using three adsorption models. The results are shown in table 1 and fig. 10 enhanced surface temperatures promoted adsorption, as evidenced by the enhanced adsorption capabilities for CR that CS/ZnO displayed at higher temperatures. This may be result of the comparatively high energy needed to overcome the barriers during adsorption in order to diffuse substantial volumes of CR molecules in the CS/ZnO pores[34]. A multilayer adsorption process was indicated by the coefficient of determination ($R^2$) value for the experimentally observed adsorption capacities of the CS/ZnO composite being larger for the Freundlich-adsorption-model, as per the data shown in table 1. Therefore, chemisorption was a major factor in the CE adsorption process by the CS/ZnO composite; the T-K model's fitting results further support this idea[42].

The efficiency of an adsorbent is directly related to its capacity to accomplish quick adsorption and quick equilibrium, especially when it comes to wastewater treatment. The purpose of this study was to investigate the effects of interaction time duration on CR dye adsorption dynamics. The efficiency of adsorbent and possibility of scaling up operations can be determined by analyzing the adsorption kinetics[17,18]. Optimizing the design of adsorption study requires a precise evaluation of the adsorption kinetics of CR dye on ZnO/CS.

Therefore, we have used two different kinetics models to better understand the process's kinetics: (1) determining whether chemical or physical mechanisms are primarily responsible for the adsorption and (2) to identify the important rate controlling step. These include pseudo second order (PSO) kinetics model[15] and pseudo first order (PFO) kinetics model[19]. It is clear from the results that the PSO model matches the empirical adsorption data very well, as evidenced by the higher $R^2$ values. This finding strongly implies that PSO model captures more accurately the adsorption of dye onto CS/ZnO. Therefore, it can be concluded that chemisorption processes are largely responsible for the adsorption of the dye by CS/ZnO[10].

We examined the CS/ZnO adsorption thermodynamics for CR at various temperatures (Fig. 12). Gibbs free energy change ($\Delta G^\circ$), entropy change ($\Delta S^\circ$) and enthalpy change ($\Delta H^\circ$) were measured. The CR adsorption by CS/ZnO was both feasible and spontaneous, as indicated by the negative $\Delta G^\circ$[6]. The increase in randomness during the CR adsorption process is reflected in the positive value of $\Delta S^\circ$[21]. The fact that adsorption study is endothermic, as showed by positive $\Delta H^\circ$, shows that adsorption-capacity of CR by CS/ZnO increases as the temperature rises[32].

**Adsorption mechanism:** The adsorption mechanism can be elucidated by analyzing interaction between surface functional group of adsorbent and Congo red. The surface of CS/ZnO contains ZnO nanoparticles (NPs) along with functional groups from chitosan (CS). Key chemical interactions involved in the adsorption of CR dye comprise of hydrogen bonding, metal-coordination and π–π interactions. Potential interaction sites on CR dye include C–N, $–NH_2$ and S=O groups. Hydrogen bonding may occur among protonated amine groups on composite surface and the $–SO_3–$ groups in Congo red dye structure. Additionally, electron donor-acceptor interactions play a significant role, as CR acts as a π-electron acceptor due to the presence of sulfonate ($–SO_3–$) groups, which are strong electron withdrawing moieties.

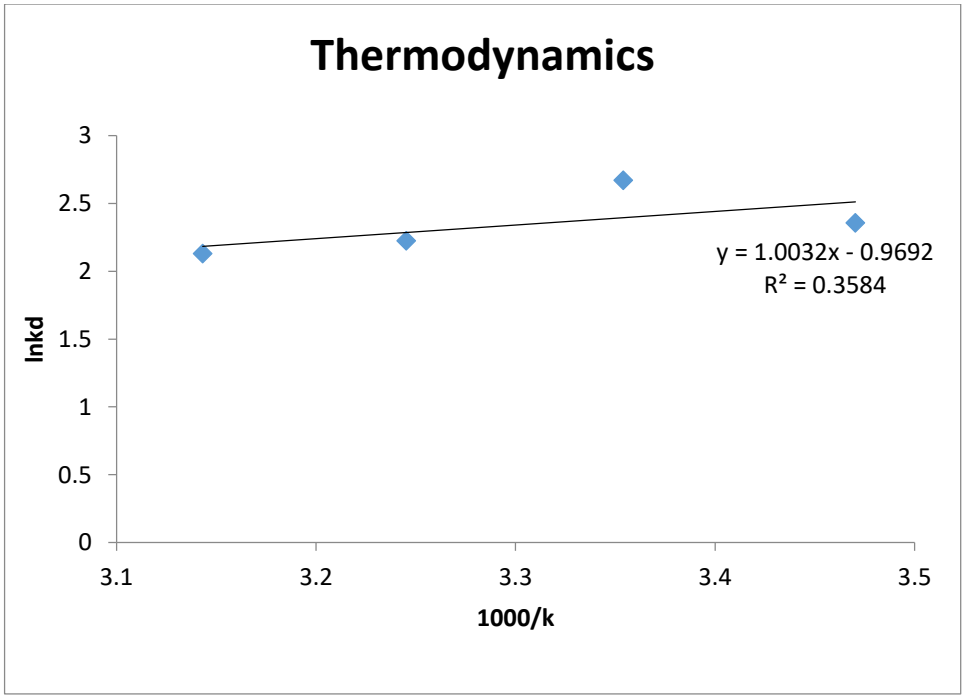


**Figure 12: Van't Hoff plots**

**Table 2**
**Thermodynamic Parameters of congo red Adsorption**

| Parameters | Values |
|---|---|
| $\Delta S^{\circ}$ | 0.008 KJ/mol |
| $\Delta H^{\circ}$ | -8.3406KJ/mol |
| $\Delta G^{\circ}$ 288K | -23.7072 KJ/mol |
| $\Delta G^{\circ}$ 298K | -24.5072 KJ/mol |
| $\Delta G^{\circ}$ 308K | -25.3072 KJ/mol |
| $\Delta G^{\circ}$ 318K | -26.1072 KJ/mol |

Furthermore, metal coordination among $-NH_2$ groups of Congo red and ZnO-NP on the composite surface contributes significantly to the adsorption process. These interactions collectively enhance the adsorption efficiency of the composite.[44]

The CS/ZnO offers a cost-effective and environmentally friendly solution for Congo red (CR) dye adsorption in wastewater treatment. These NPs demonstrate excellent adsorption properties, with the CS/ZnO outperforming due to the enhanced functionality provided by ZnO nanoparticles. While composite is mainly effective in removing Congo red dye, its versatility suggests potential applicability for the removal of other organic anionic-dyes, broadening its utility in water treatment processes. The scalability of the fabrication process further highlights its potential for large-scale industrial wastewater treatment applications. However, certain limitations must be addressed before commercialization.

The dye removal efficiency can vary depending on fabrication parameters and operational condition, necessitating optimization for consistent performance. Additionally, the environmental impact of the NPs, including its disposal after use, must be carefully evaluated to ensure sustainability. Addressing these challenges will be crucial for the successful implementation of this technology in real-world wastewater treatment systems.

## Conclusion

The ZnO based chitosan nanocomposite was effectively produced in this study using a simple, quick and environment friendly *in situ* precipitation approach. The nanocomposite possesses a wurtzite structure, according to the XRD measurements. The nanocomposite is around 70–75 nm in size. The material's spherical form is visible in the FE-SEM micrographs. The congo red was extracted from aqueous solutions using the ZnO/chitosan nanocomposite material as an adsorbent. The ZnO/chitosan nanocomposite has a theoretical maximum adsorption capacity of 92.59 (mg/g) based on the Langmuir isotherm model.

The finding implies that the ZnO/chitosan nanocomposite may be a potential congo red adsorbent in wastewater treatment technology. It helps to create effective and long-lasting adsorption processes by offering insightful information about the intricate relationships between dye molecules and adsorbent materials.

## Acknowledgement

Authors acknowledge UIET and CIL, M.D.University for instrumentation facilities and UGC for JRF fellowship.

## References

1. Ahmad R. and Mirza A., Inulin-folic acid/bentonite: a novel nanocomposite for confiscation of Cu (II) from synthetic and industrial wastewater, *Journal of Molecular Liquids*, **241**, 489-499 **(2017)**

2. Alsawat M., Congo Red Dye Adsorption using $CuSnO_2TiO_2$ Nanocomposites: Adsorption Data Interpretation by Statistical Modeling, *International Journal of Electrochemical Science*, **19(7)**, 100611 **(2024)**

3. Ansari S.A., Ansari S.G., Foaud H. and Cho M.H., Facile and sustainable synthesis of carbon-doped ZnO nanostructures towards the superior visible light photocatalytic performance, *New Journal of Chemistry*, **41(17)**, 9314-9320 **(2017)**

4. Badawy M.S.E., Riad O.K.M., Taher F.A. and Zaki S.A., Chitosan and chitosan-zinc oxide nanocomposite inhibit expression of LasI and RhlI genes and quorum sensing dependent virulence factors of Pseudomonas aeruginosa, *International Journal of Biological Macromolecules*, **149**, 1109-1117 **(2020)**

5. Bharathi D., Ranjithkumar R., Chandarshekar B. and Bhuvaneshwari V., Preparation of chitosan coated zinc oxide nanocomposite for enhanced antibacterial and photocatalytic activity: As a bionanocomposite, *International Journal of Biological Macromolecules*, **129**, 989-996 **(2019)**

6. Cui Y., Kang W., Qin L., Ma J., Liu X. and Yang Y., Magnetic surface molecularly imprinted polymer for selective adsorption of quinoline from coking wastewater, *Chemical Engineering Journal*, **397**, 125480 **(2020)**

7. Dananjaya S.H.S., Kumar R.S., Yang M., Nikapitiya C., Lee J. and De Zoysa M., Synthesis, characterization of ZnO-chitosan nanocomposites and evaluation of its antifungal activity against pathogenic *Candida albicans*, *International Journal of Biological Macromolecules*, **108**, 1281-1288 **(2018)**

8. Deng Q., Wang X., Shao M., Fang L., Zhao X., Xu J. and Wang X., Synthesis of chitosan-modified magnetic metal-organic framework and its adsorption of Congo red and antibacterial activity, *Microporous and Mesoporous Materials*, **342**, 112042 **(2022)**

9. Deng X., Wu W., Tian S., He Y., Wang S., Zheng B., Xin K., Zhou Z. and Tang L., Composite adsorbents of aminated chitosan @ZIF-8 MOF for simultaneous efficient removal of Cu(II) and

Congo Red: Batch experiments and DFT calculations, *Chemical Engineering Journal*, **479**, 147634 **(2023)**

10. Doondani P., Panda D., Gomase V., Peta K.R. and Jugade R., Novel Chitosan-ZnO nanocomposites derived from Nymphaeaceae fronds for highly efficient removal of Reactive Blue 19, Reactive Orange 16 and Congo Red dyes, *Environmental Research*, **247**, 118228 **(2024)**

11. Dubinin M.M., Porous structure and adsorption properties of active carbons, *Chemistry and Physics of Carbon*, **9**, 51-119 **(1966)**

12. Foroughi M., Peighambardoust S.J., Ramavandi B., Foroutan R. and Peighambardoust N.S., Simultaneous degradation of methyl orange and indigo carmine dyes from an aqueous solution using nanostructured WO3 and CuO supported on Zeolite 4A, *Separation and Purification Technology*, **344**, 127265 **(2024)**

13. Gopalakrishnan S., Kannan P., Balasubramani K., Rajamohan N. and Rajasimman M., Sustainable remediation of toxic congo red dye pollution using bio based carbon nanocomposite: Modelling and performance evaluation, *Chemosphere*, **343**, 140206 **(2023)**

14. Harja M., Buema G. and Bucur D., Recent advances in removal of Congo Red dye by adsorption using an industrial waste, *Scientific Reports*, **12(1)**, 1-18 **(2022)**

15. Ho Y.S. and McKay G., Sorption of dye from aqueous solution by peat, *Chemical Engineering Journal*, **70(2)**, 115-124 **(1998)**

16. Jawad A.H., Rangabhashiyam S., Abdulhameed A.S., Syed-Hassan S.S.A., ALOthman Z.A. and Wilson L.D., Process optimization and adsorptive mechanism for reactive blue 19 dye by magnetic crosslinked chitosan/MgO/$Fe_3O_4$ biocomposite, *Journal of Polymers and the Environment*, **30(7)**, 2759-2773 **(2022)**

17. Jawad A.H., Saber S.E.M., Abdulhameed A.S., Reghioua A., ALOthman Z.A. and Wilson L.D., Mesoporous activated carbon from mangosteen (Garcinia mangostana) peels by $H_3PO_4$ assisted microwave: Optimization, characterization and adsorption mechanism for methylene blue dye removal, *Diamond and Related Materials*, **129**, 109389 **(2022)**

18. Jiang R., Zhu H.Y., Fu Y.Q., Zong E.M., Jiang S.T., Li J.B. and Zhu Y.Y., Magnetic $NiFe_2O_4$/MWCNTs functionalized cellulose bioadsorbent with enhanced adsorption property and rapid separation, *Carbohydrate Polymers*, **252**, 117158 **(2021)**

19. Karaningannavar Shwetha, Hegde Rajat and Yarajarla Ramesh Babu, Simple and Rapid PCR-RFLP based species identification in Drosophila suzukii and Drosophila immigrans larvae, *Res. J. Biotech.*, **19(3)**, 48-50 **(2024)**

20. Langmuir I., The adsorption of gases on plane surfaces of glass, mica and platinum, *Journal of the American Chemical Society*, **40(9)**, 1361-1403 **(1918)**

21. Liu D.M., Dong C., Zhong J., Ren S., Chen Y. and Qiu T., Facile preparation of chitosan modified magnetic kaolin by one-pot coprecipitation method for efficient removal of methyl orange, *Carbohydrate Polymers*, **245**, 116572 **(2020)**

22. Manubolu M., Pathakoti K. and Leszczynski J., Recent advances in chitosan-based nanocomposites for dye removal: a review, *International Journal of Environmental Science and Technology*, **21(4)**, 4685-4704 **(2024)**

23. Mostafa M.H., Elsawy M.A., Darwish M.S., Hussein L.I. and Abdaleem A.H., Microwave-Assisted preparation of Chitosan/ ZnO nanocomposite and its application in dye removal, *Materials Chemistry and Physics*, **248**, 122914 **(2020)**

24. Peighambardoust S.J., Boffito D.C., Foroutan R. and Ramavandi B., Sono-photocatalytic activity of sea sediment@ 400/ ZnO catalyst to remove cationic dyes from wastewater, *Journal of Molecular Liquids*, **367**, 120478 **(2022)**

25. Preethi S., Abarna K., Nithyasri M., Kishore P., Deepika K., Ranjithkumar R., Bhuvaneshwari V. and Bharathi D., Synthesis and characterization of chitosan/zinc oxide nanocomposite for antibacterial activity onto cotton fabrics and dye degradation applications, *International Journal of Biological Macromolecules*, **164**, 2779-2787 **(2020)**

26. Rajashekaraiah R., Kumar P.R., Prakash N., Rao G.S., Devi V.R., Metta M. and Govindappa P.K., Anticancer efficacy of 6-thioguanine loaded chitosan nanoparticles with or without curcumin, *International Journal of Biological Macromolecules*, **148**, 704-714 **(2020)**

27. Raval N.P., Priyadarshi G.V., Mukherjee S., Zala H., Fatma D., Bonilla-Petriciolet A., Abdelmottaleb B.L., Duclaux L. and Trivedi M.H., Statistical physics modeling and evaluation of adsorption properties of chitosan-zinc oxide nanocomposites for the removal of an anionic dye, *Journal of Environmental Chemical Engineering*, **10(6)**, 108873 **(2022)**

28. Razmi F.A., Ngadi N., Wong S., Inuwa I.M. and Opotu L.A., Kinetics, thermodynamics, isotherm and regeneration analysis of chitosan modified pandan adsorbent, *Journal of Cleaner Production*, **231**, 98-109 **(2019)**

29. Roy H., Islam M.S., Arifin M.T. and Firoz S.H., Synthesis, Characterization and Sorption Properties of Biochar, Chitosan and ZnO-Based Binary Composites towards a Cationic Dye, *Sustainability*, **14(21)**, 14571 **(2021)**

30. Salahshoori I., Wang Q., Nobre M.A., Mohammadi A.H., Dawi E.A. and Khonakdar H.A., Molecular simulation-based insights into dye pollutant adsorption: a perspective review, *Advances in Colloid and Interface Science*, https://doi.org/10.1016/ j.cis.2024.103281 **(2024)**

31. Sharma P., Sharma M., Yadav L., Agarwal M. and Gupta R., Sustainable solution for wastewater management: Fabrication of cost-effective β-cyclodextrin incorporated chitosan polyvinyl alcohol composite hydrogel film for the efficient adsorption of anionic congo red and tartrazine dyes, *Separation and Purification Technology*, **355**, 129750 **(2025)**

32. Shuyue J., Dongyan T., Jing P., Xu Y. and Zhaojie S., Cross linked electrospinning fibers with tunable swelling behaviors: A novel and effective adsorbent for Methylene Blue, *Chemical Engineering Journal*, **390**, 124472 **(2020)**

33. Umesh A.S., Puttaiahgowda Y.M. and Thottathil S., Enhanced adsorption: Reviewing the potential of reinforcing polymers and hydrogels with nanomaterials for methylene blue dye removal, *Surfaces and Interfaces*, **51**, 104670 **(2024)**

34. Wei J., Liu Y., Li J., Zhu Y., Yu H. and Peng Y., Adsorption and co-adsorption of tetracycline and doxycycline by one-step synthesized iron loaded sludge biochar, *Chemosphere*, **236**, 124254 **(2019)**

35. Wu H. and Zhang, Chitosan-based zinc oxide nanoparticle for enhanced anticancer effect in cervical cancer: A physicochemical and biological perspective, *Saudi Pharmaceutical Journal*, **26(2)**, 205-210 **(2018)**

36. Yadav S. et al, Assessment of groundwater quality near municipal solid waste landfill by using multivariate statistical technique and GIS: a case study of Bandhwari (Gurugram) landfill site, Haryana, India, *Sustain. Water Resour. Manag.*, **9**, 174 **(2023)**

37. Yadav S., Dhankhar R. and Chhikara S.K., Significant Changes in Urban Air Quality during Covid-19 Pandemic Lockdown in Rohtak City, India, *Asian J Chem*, **34(12)**, 3189-3196 **(2022)**

38. Yadav S., Rohilla R. and Chhikara S.K., Review on Landfill Leachate Treatment: Focus on the Applicability of Adsorbents, Proc. Natl. Acad. Sci., India, Sect. B Biol. Sci. **(2024)**

39. Yadav S., Yadav A., Goyal G., Dhawan M., Kumar V., Yadav A., Dhankhar R., Sehrawat N. and Chhikara S.K., Fly Ash-based Adsorption for Hexavalent Chromium Removal in Aqueous Systems: A Promising Eco-Friendly Technique, *Oriental Journal of Chemistry*, **40(1)**, 182 **(2024)**

40. Yardımcı B. and Kanmaz N., Ecosafe-design of carboxymethyl cellulose encapsulated polyphenolic bio-nanocomposite valorized for sustainable industrial textile dye removal, *Journal of Environmental Chemical Engineering*, DOI: 10.1016/j.jece.2025. 115321 **(2025)**

41. Yusof N.A.A., Zain N.M. and Pauzi N., Synthesis of ZnO nanoparticles with chitosan as stabilizing agent and their antibacterial properties against Gram-positive and Gram-negative bacteria, *International Journal of Biological Macromolecules*, **124**, 1132-1136 **(2019)**

42. Zhang S., Liu C., Yuan Y., Fan M., Zhang D., Wang D. and Xu Y., Selective, highly efficient extraction of Cr (III), Pb (II) and Fe (III) from complex water environment with a tea residue derived porous gel adsorbent, *Bioresource Technology*, **311**, 123520 **(2020)**

43. Zheng Y., Cheng B., Fan J., Yu J. and Ho W., Review on nickel-based adsorption materials for Congo red, *Journal of Hazardous Materials*, **403**, 123559 **(2021)**.

(Received 17th January 2025, accepted 22nd March 2025)